SANDIA REPORT

SAND2001-0044
Unlimited Release
Printed January 2001

Performance Limits for Synthetic Aperture Radar

Armin W. Doerry

Prepared by
Sandia National Laboratories
Albuquerque, New Mexico 87185 and Livermore, California 94550

Sandia is a multiprogram laboratory operated by Sandia Corporation, a Lockheed Martin Company, for the United Sates Department of Energy under Contract DE-AC04-94AL85000.

Sandia National Laboratories

Issued by Sandia National Laboratories, operated for the United States Department of Energy by Sandia Corporation.

Available to DOE and DOE contractors from
U.S. Department of Energy
Office of Scientific and Technical Information
P.O. Box 62
Oak Ridge, TN 37831

Telephone: (865) 576-8401
Facsimile: (865) 576-5728
E-Mail: reports@adonis.osti.gov
Online ordering: http://www.doe.gov/bridge

Available to the public from
U.S. Department of Commerce
National Technical Information Service
5285 Port Royal Rd
Springfield, VA 22161

Telephone: (800) 553-6847
Facsimile: (703) 605-6900
E-Mail: orders@ntis.fedworld.gov
Online ordering: http://www.ntis.gov/ordering.htm

SAND2001-0044
Unlimited Release
Printed January 2001

Performance Limits for Synthetic Aperture Radar

Armin W. Doerry
Synthetic Aperture Radar Department
Sandia National Laboratories
PO Box 5800
Albuquerque, NM 87109-0519

ABSTRACT

The performance of a Synthetic Aperture Radar (SAR) system depends on a variety of factors, many which are interdependent in some manner. It is often difficult to ‘get your arms around’ the problem of ascertaining achievable performance limits, and yet those limits exist and are dictated by physics, no matter how bright the engineer tasked to generate a system design. This report identifies and explores those limits, and how they depend on hardware system parameters and environmental conditions. Ultimately, this leads to a characterization of parameters that offer optimum performance for the overall SAR system.

For example, there are definite optimum frequency bands that depend on weather conditions and range, and minimum radar PRF for a fixed real antenna aperture dimension is independent of frequency.

While the information herein is not new to the literature, its collection into a single report hopes to offer some value in reducing the ‘seek time’.

ACKNOWLEDGEMENTS

This work was funded in part by US DOE Office of Nonproliferation & National Security, Office of Research & Development. This effort was supervised by Randy Bell of DOE.

Sandia is a multiprogram laboratory operated by Sandia Corporation, a Lockheed Martin Company, for the United States Department of Energy under Contract DE-AC04-94AL85000.

CONTENTS

1. Introduction

Synthetic Aperture Radar (SAR) performance is dependent on a multitude of parameters, many of which are interrelated in non-linear fashions. Seemingly simple questions such as "What range can we operate at?", "What resolution can we get?", "How fast can we fly?", and "What frequency should we operate at?", are often (and rightly so) hesitantly answered with a slew of qualifiers (ifs, buts, givens, etc.).

These invariably result in performance studies that trade various parameters against each other. Nevertheless, general trends can be observed, and general statements can be made. Furthermore, performance bounds can be generated to offer first order estimates on the achievability of various performance goals. This report attempts to do just this.

2. The Radar Equation

The performance measure is Signal-to-Noise (energy) Ratio (SNR) in the SAR image. A brief recap on the development of this equation is as follows.

For a single pulse, the Received (RX) power at the antenna port is related to the Transmitted (TX) power by

$$P_r = P_t G_A \left(\frac{1}{4\pi |\boldsymbol{r}_c|^2} \right) \sigma \left(\frac{1}{4\pi |\boldsymbol{r}_c|^2} \right) A_e = \frac{P_t G_A A_e \sigma}{(4\pi)^2 |\boldsymbol{r}_s|^4 L_{\text{radar}} L_{\text{atmos}}}, \tag{1}$$

where

P_r = received signal power (W),

P_t = transmitter signal power (W),

G_A = transmitter antenna gain factor,

A_e = receiver antenna effective area (m^2),

σ = target Radar Cross Section (m^2),

$\boldsymbol{r}_s$ = range vector from target to antenna (m),

L_{atmos} = atmospheric loss factor due to the propagating wave,

L_{radar} = microwave transmission loss factor due to miscellaneous sources. (2)

The noise power that the signal must compete with at the antenna is given approximately by

$$N_r = kTF_N B, \tag{3}$$

where

N_r = received noise power (W),

k = Boltzmann's constant = 1.38 x 10-23 J/K,

T = nominal scene noise temperature ≈ 290 K,

F_N = system noise factor for the receiver,
B = noise bandwidth at the antenna port. (4)

Consequently, the Signal-to-Noise (power) ratio at the RX antenna port is

$$\mathrm{SNR}_{\mathrm{antenna}} = \frac{P_r}{N_r} = \frac{P_t G_A A_e \sigma}{(4\pi)^2 |\boldsymbol{r}_s|^4 L_{\mathrm{radar}} L_{\mathrm{atmos}} (kTF_N) B}. \quad (5)$$

A finite data collection time limits the total energy collected, and signal processing in the radar increases the SNR in the SAR image by two major gain factors. This results in

$$\mathrm{SNR}_{\mathrm{image}} = \mathrm{SNR}_{\mathrm{antenna}} \left(\frac{G_r G_a}{L_{\mathrm{sp}}} \right) = \frac{P_t G_A A_e \sigma G_r G_a}{(4\pi)^2 |\boldsymbol{r}_s|^4 L_{\mathrm{radar}} L_{\mathrm{atmos}} L_{\mathrm{sp}} (kTF_N) B}, \quad (6)$$

where

G_r = SNR gain due to range processing (pulse compression),
G_a = SNR gain due to azimuth processing (coherent pulse integration),
L_{sp} = SNR loss due to a variety of signal processing issues. (7)

This relationship is called “The Radar Equation”.

At this point we examine the image SNR terms and factors individually to relate them to physical SAR system parameters and performance criteria.

2.1. Antenna

This report will consider only the monostatic case, where the same antenna is used for TX and RX operation. Consequently, we relate

$$G_A = \frac{4\pi A_e}{\lambda^2}, \quad (8)$$

where λ is the nominal wavelength of the radar. Furthermore, the effective area is related to the actual aperture area by

$$A_e = \eta_{\mathrm{ap}} A_A, \quad (9)$$

where

η_{ap} = the aperture efficiency of the antenna,
A_A = the physical area of the antenna aperture. (10)

Typically, a radar design must live with a finite volume for the antenna structure, so that the achievable antenna physical aperture area is limited. The aperture efficiency takes into account a number of individual efficiency factors, including the radiation efficiency of the antenna, the aperture illumination efficiency of say a feedhorn to a reflector assembly,

spillover losses of a feedhorn to a finite reflector area, etc. A typical number for aperture efficiency might be $\eta_{ap} \approx 0.5$.

Putting these into the radar equation yields

$$\mathrm{SNR}_{\mathrm{image}} = \frac{P_t(\eta_{\mathrm{ap}}^2 A_A^2)\sigma G_r G_a}{(4\pi)|\boldsymbol{r}_s|^4 \lambda^2 L_{\mathrm{radar}} L_{\mathrm{atmos}} L_{\mathrm{sp}} (kTF_N) B}. \tag{11}$$

2.2. Processing gains

The range processing gain is due to bandwidth reduction and pulse compression. It is straightforward to show that

$$G_r = \frac{T_{eff} B}{a_w}, \tag{12}$$

where

T_{eff} = the effective pulse width of the radar, and

a_w = normalized bandwidth of signal processing window functions. (13)

A typical window function bandwidth is on the order of $a_w \approx 1.2$.

The effective pulse width differs from the actual TX pulse width in that the effective pulse width is equal to that portion of the real pulse that makes it into the data set. For digital matched-filter processing they are the same, but for stretch-processing the effective pulse width is typically slightly less than the real transmitted pulse width, but still pretty close. For the remainder of this report we will presume that the transmitted pulse width is equal to the effective pulse width.

The azimuth processing gain is due to the coherent integration of multiple pulses, whether by presumming or actual Doppler processing. Of course, the total number of pulses that can be collected depends on the radar PRF and the time it takes to fly the aperture, which in turn depends on platform velocity and the physical dimension of the synthetic aperture, which in turn depends on the azimuth resolution desired. Assuming a broadside collection geometry, and putting all this together yields

$$G_a = \frac{N}{a_w} = \frac{f_p \lambda |\boldsymbol{r}_s|}{2\rho_a v_x}, \tag{14}$$

where

f_p = radar PRF (Hz),

ρ_a = image azimuth resolution (m),

v_x = platform velocity (m/s), horizontal and orthogonal to $|\boldsymbol{r}_s|$. (15)

Putting these into the radar equation yields

$$\mathrm{SNR}_{\mathrm{image}} = \frac{P_t T_{eff} f_p (\eta_{\mathrm{ap}}^2 A_A^2) \sigma}{2(4\pi) v_x |\boldsymbol{r}_s|^3 \lambda \rho_a a_w L_{\mathrm{radar}} L_{\mathrm{atmos}} L_{\mathrm{sp}} (kTF_N)}. \tag{16}$$

2.3. The Transmitter

The transmitter is generally specified to first order by 3 main criteria:

1) The frequency range of operation,

2) The peak power output (averaged during the pulse on-time), and

3) The maximum duty factor allowed.

We identify the duty factor as

$$d = T_{eff} f_p = \frac{P_{\mathrm{avg}}}{P_t}, \tag{17}$$

where P_{avg} is the average power transmitted during the synthetic aperture data collection period. Consequently, we identify

$$P_t T_{eff} f_p = P_t d = P_{\mathrm{avg}}. \tag{18}$$

Transmitter power capabilities and bandwidths are very dependent on transmitter technology. In general, for tube-type power amplifiers, higher power generally implies lesser capable bandwidth, and hence lesser range resolution. The bandwidth required for a particular range resolution *for a single pulse* is given by

$$B = \frac{a_w c}{2\rho_r}, \tag{19}$$

where

ρ_r = slant-range resolution required,

c = velocity of propagation. (20)

There is no typical duty factor that characterizes all, or even most, power amplifiers. Duty factors may range from on the order of 1% to 100% across the variety of power amplifiers available. Typically, a maximum duty factor needed by a radar is less than 50%, and usually less than about 35% or so. Consequently, a reasonable duty factor limit of 35% might be imposed on power amplifiers that could otherwise be capable of more.

In practice, the duty factor limit for a particular power amplifier may not always be achieved due to timing constraints for the geometry within which the radar is operating, but we can often get pretty close.

We take this opportunity to also note that

$$\lambda = c/f, \tag{21}$$

where *f* is the radar nominal frequency.

Power Amplifier Tubes

The following table indicates some representative power amplifier tube capabilities.

Table 1: Power Amplifier Tubes

Power Amplifier Tube	*Frequency Band of Operation (GHz)*	Peak Power (W)	Max Duty Factor	Avg Power (W)
CPI VTU-5010W2	15.2 - 18.2	320	0.35	112
Teledyne MEC 3086	15.5 - 17.9	700	0.35	245
Litton L5869-50	16.25 - 16.75	4000	0.30	1200
Teledyne MTI 3048D	8.7 - 10.5	4000	0.10	400
CPI VTX-5010E	7.5 - 10.5	350	0.35	123
Teledyne MTI3948R	8.7 - 10.5	7000	0.07	490
Litton L5806-50	9.0 - 9.8	9000	0.50	3150[a]
Litton L5901-50	9.6 - 10.2	20000	0.06	1200
Litton L5878-50	5.25 - 5.75	60000	0.035	2100
Teledyne MEC 3082	3.0 - 4.0	10000	0.04	400

a. based on 0.35 maximum duty factor

Solid-State Amplifiers

Solid-state power amplifiers are generally lower in power than their tube counterparts, typically under 100 W, and more likely in the 10 W to 20 W range (depending on frequency band). However, they do offer a possible efficiency advantage, and technology is advancing to the point where these should be considered for relatively short range radar applications.

Electronic Phased-Arrays

An alternative to power amplifier tubes is an electronic Active Phased Array (APA), made up of many small, relatively low-power (generally solid-state) Transmit/Receive (T/R) modules. This is a scalable architecture that spatially combines the power from many individual elements. Current state-of-the-art is approaching 10 W of power from an X-band T/R module with 1 cm^2 cross section. This represents an aperture power density of 100 kW/m^2. That is, heat dissipation problems notwithstanding, a rather small antenna aperture of 0.1 m^2 could possibly radiate 10 kW of peak power with a relatively high duty factor. New technologies such as GaN offer the promise of many tens of Watts at higher frequencies (Ku-band and even Ka-band) from a single MMIC. Furthermore, an Electronically Steerable Array (ESA) doesn't require a gimbal assembly for pointing, and could conceivably allow a larger aperture area for a given antenna assembly volume constraint.

In any case, we refine the radar equation to be

$$\mathrm{SNR}_{\mathrm{image}} = \frac{P_{\mathrm{avg}}(\eta_{\mathrm{ap}}^2 A_A^2) f\sigma}{2(4\pi)cv_x|\boldsymbol{r}_s|^3 \rho_a a_w L_{\mathrm{radar}} L_{\mathrm{atmos}} L_{\mathrm{sp}} (kTF_N)}, \tag{22}$$

noting that the average power is based on the power amplifier's duty factor limit, or perhaps 35%, whichever is less.

2.4. The Target Radar Cross Section (RCS)

The RCS of a target denotes its ability to reflect energy back to the radar. For SAR, the target of interest in terms of radar performance is generally a distributed target, such as grass, corn fields, etc. For these target types, the RCS is dependent on the area being resolved. Consequently, for distributed targets, RCS is generally specified as a reflectivity number that normalizes RCS per unit area. The actual area is the area of a resolution cell, as projected on the ground. Consequently

$$\sigma = \sigma_0 \rho_a \left(\frac{\rho_r}{\cos\psi} \right), \tag{23}$$

where

$$\begin{aligned} &\sigma_0 = \text{distributed target reflectivity } (\mathrm{m}^2/\mathrm{m}^2), \\ &\psi = \text{grazing angle at the target location.} \end{aligned} \tag{24}$$

In addition, σ_0 is generally frequency-dependent, typically proportional to f^n, where n depends on target type, with $0 < n < 1$, but usually closer to 1.[5] Consequently we can write

$$\sigma = \sigma_{0,\,\mathrm{ref}} \left(\frac{\rho_a \rho_r}{\cos\psi} \right) \left(\frac{f}{f_{\mathrm{ref}}} \right)^n, \tag{25}$$

where $\sigma_{0,\,\mathrm{ref}}$ is the reflectivity of interest at nominal reference frequency f_{ref}. At this point, target RCS embodies a frequency dependence, as it should.

We note that even for non-distributed targets, a variety of frequency dependencies exists, and are characterized in the following table.

Table 2: RCS frequency dependence.

target characteristic	*examples*	frequency dependence
2 radii of curvature	spheroids	none
1 radius of curvature	cylinders, top hats	f
0 radii of curvature	flat plates, dihedrals, trihedrals	f^2

A typical radar specification requires a SNR of 0 dB for a target reflectivity of –25 dB at Ku-band (nominally 16.7 GHz). This corresponds to $\sigma_{0,\,\mathrm{ref}} = -25$ dB, with $f_{\mathrm{ref}} = 16.7$ GHz. The implication is that the same target scene would be dimmer at lower frequencies, and brighter at higher frequencies.

Additionally, $\sigma_{0,\,\mathrm{ref}}$ will exhibit some dependency itself on grazing angle ψ. This dependency is sometimes incorporated into a model known as 'constant-γ' reflectivity model. Other times the grazing angle dependence is just ignored.

Nevertheless, folding the RCS dependencies into the radar equation, and rearranging a bit, yields

$$\mathrm{SNR}_{\mathrm{image}} = \frac{P_{\mathrm{avg}}(\eta_{\mathrm{ap}}^2 A_A^2)\rho_r\left(\dfrac{\sigma_{0,\,\mathrm{ref}}}{f_{\mathrm{ref}}^n}\right)(f)^{n+1}}{(8\pi)a_w c(kTF_N)v_x \cos\psi |\boldsymbol{r}_s|^3 L_{\mathrm{sp}} L_{\mathrm{radar}} L_{\mathrm{atmos}}}. \tag{26}$$

2.5. Radar Geometry

Typically, the radar is specified to operate at a particular height. Consequently, grazing angle depends on this height and the slant-range of operation. That is,

$$\sin\psi = h/|\boldsymbol{r}_s|, \tag{27}$$

or

$$\cos\psi = \sqrt{1-(h/|\boldsymbol{r}_s|)^2}, \tag{28}$$

where h = the height of the radar above the target.

This yields a radar equation as follows,

$$\mathrm{SNR}_{\mathrm{image}} = \frac{P_{\mathrm{avg}}(\eta_{\mathrm{ap}}^2 A_A^2)\rho_r\left(\dfrac{\sigma_{0,\,\mathrm{ref}}}{f_{\mathrm{ref}}^n}\right)(f)^{n+1}}{(8\pi)a_w c(kTF_N)v_x |\boldsymbol{r}_s|^3 \sqrt{1-(h/|\boldsymbol{r}_s|)^2} L_{\mathrm{sp}} L_{\mathrm{radar}} L_{\mathrm{atmos}}}. \tag{29}$$

2.6. SNR Losses and Noise Factor

The radar equation as presented notes several broad categories of SNR losses.

Signal Processing Loss

These include the SNR loss (relative to ideal processing gains) due to employing a window

function. Recall that the window bandwidth (including its noise bandwidth) is increased somewhat. If window functions are incorporated in both dimensions (range and azimuth processing), then we incur a SNR loss typically on the order of 1 dB for each dimension, or perhaps 2 dB overall.

If a target of interest is other than distributed, we might also incorporate a 'straddling' loss due to a target not being centered in a resolution cell. This depends on the relationship of pixel spacing to resolution, also known as the oversampling factor, but might be as high as 3 dB. For distributed targets, being off-center of a resolution cell is meaningless.

Radar Losses

These include a variety of losses primarily over the microwave signal path, but doesn't include the atmosphere. Included are a power loss from transmitter power amplifier output to the antenna port, and a two-way loss thru the radome. These are generally somewhat frequency dependent, being higher at higher frequencies, but major effort is expended to keep them both as low as is reasonably achievable. In the absence of more refined information, typical numbers might be 0.5 dB to 2 dB from TX amplifier to the antenna port, and perhaps an additional 0.5 dB to 1.5 dB two-way thru the radome.

System Noise Factor

When this number is expressed in dB, it is often referred to as the system noise figure.

The system noise figure includes primarily the noise figure of the front-end Low-Noise Amplifier (LNA) and the losses between the antenna and the LNA. These both are a function of a variety of factors, including the length and nature of cables required, LNA protection and isolation requirements, and of course frequency. Frequency dependence is generally such that higher frequencies will result in higher system noise figures. For example, typical system noise figures for sub-kilowatt radar systems are 3.0 dB to 3.5 dB at X-band, 3.5 dB to 4.5 dB at Ku-band, and perhaps 6 dB at Ka-band.

Atmospheric Losses

Atmospheric losses depend strongly on frequency, range, and the nature of the atmosphere (particularly the weather conditions) between radar and target. Major atmospheric loss factors are atmospheric density, humidity, cloud water content, and rainfall rate. These conspire to yield a 'loss-rate' often expressed as dB per unit distance, that is very altitude and frequency dependent. The loss-rate generally increases strongly with frequency, but decreases with radar altitude, owing to the signal path traversing a thinner average atmosphere.

A typical radar specification is to yield adequate performance in an atmosphere that includes weather conditions supporting a 4 mm/Hr rainfall rate on the ground.

We identify the overall atmospheric loss as

$$L_{\text{atmos}} = 10^{\frac{\alpha |\boldsymbol{r}_s|}{10}}, \tag{30}$$

where α = the two-way atmospheric loss rate in dB per unit distance.

Nominal two-way loss rates from various altitudes for some surface rain rates are listed in the following tables. While numbers listed are to several significant digits, these are based on a model and are quite squishy.[1]

Incorporating atmospheric loss-rate overtly into the radar equation, and rearranging a bit, yields

$$\mathrm{SNR}_{\mathrm{image}} = \frac{P_{\mathrm{avg}}(\eta_{\mathrm{ap}}^2 A_A^2)\rho_r \left(\frac{\sigma_{0,\,\mathrm{ref}}}{f_{\mathrm{ref}}^n}\right)(f)^{n+1}}{(8\pi)a_w ckTv_x(L_{\mathrm{sp}}L_{\mathrm{radar}}F_N)\left(|\boldsymbol{r}_s|^3\sqrt{1-(h/|\boldsymbol{r}_s|)^2}\,10^{\frac{\alpha|\boldsymbol{r}_s|}{10}}\right)}. \qquad (31)$$

Implicit in the radar equation is that atmospheric loss-rate α depends on f in a decidedly nonlinear manner (and not necessarily even monotonic near specific absorption bands – of note are an H_2O absorption band at about 23 GHz, and an O_2 absorption band at about 60 GHz).

Table 3: Two-way loss rates (dB/km) in 50% RH clear air

Radar Altitude (kft)	L-band 1.5 GHz	S-band 3.0 GHz	C-band 5.0 GHz	X-band 9.6 GHz	Ku-band 16.7 GHz	Ka-band 35 GHz	W-band 94 GHz
5	0.0119	0.0138	0.0169	0.0235	0.0648	0.1350	0.7101
10	0.0110	0.0126	0.0149	0.0197	0.0498	0.1053	0.5357
15	0.0102	0.0115	0.0133	0.0170	0.0400	0.0857	0.4236
20	0.0095	0.0105	0.0120	0.0149	0.0333	0.0721	0.3476
25	0.0087	0.0096	0.0108	0.0132	0.0282	0.0616	0.2907
30	0.0080	0.0088	0.0099	0.0119	0.0246	0.0541	0.2515
35	0.0074	0.0081	0.0090	0.0108	0.0218	0.0481	0.2214
40	0.0069	0.0075	0.0083	0.0099	0.0196	0.0434	0.1977
45	0.0064	0.0069	0.0076	0.0090	0.0176	0.0392	0.1774
50	0.0059	0.0064	0.0071	0.0083	0.0161	0.0360	0.1617

Table 4: Two-way loss rates (dB/km) in 4 mm/Hr (moderate) rainy weather

Radar Altitude (kft)	L-band 1.5 GHz	S-band 3.0 GHz	C-band 5.0 GHz	X-band 9.6 GHz	Ku-band 16.7 GHz	Ka-band 35 GHz	W-band 94 GHz
5	0.0135	0.0207	0.0502	0.1315	0.5176	2.1818	8.7812
10	0.0126	0.0193	0.0450	0.1107	0.4062	1.7076	7.7623
15	0.0117	0.0175	0.0391	0.0920	0.3212	1.3311	6.4537
20	0.0106	0.0150	0.0314	0.0714	0.2453	1.0082	4.8836
25	0.0096	0.0132	0.0264	0.0584	0.1979	0.8108	3.9218
30	0.0088	0.0118	0.0228	0.0496	0.1662	0.6788	3.2796
35	0.0081	0.0107	0.0201	0.0431	0.1433	0.5838	2.8178
40	0.0074	0.0098	0.0180	0.0382	0.1259	0.5122	2.4701
45	0.0069	0.0089	0.0163	0.0342	0.1121	0.4558	2.1967
50	0.0064	0.0082	0.0149	0.0310	0.1012	0.4109	1.9793

Table 5: Two-way loss rates (dB/km) in 16 mm/Hr (heavy) rainy weather

Radar Altitude (kft)	L-band 1.5 GHz	S-band 3.0 GHz	C-band 5.0 GHz	X-band 9.6 GHz	Ku-band 16.7 GHz	Ka-band 35 GHz	W-band 94 GHz
5	0.0166	0.0373	0.1531	0.4910	1.8857	7.3767	23.0221
10	0.0159	0.0347	0.1282	0.3829	1.4091	5.6330	21.0363
15	0.0146	0.0307	0.1060	0.3020	1.0738	4.3037	17.7448
20	0.0128	0.0249	0.0816	0.2289	0.8097	3.2377	13.3520
25	0.0113	0.0211	0.0665	0.1844	0.6459	2.5944	10.6964
30	0.0102	0.0184	0.0563	0.1546	0.5425	2.1651	8.9251
35	0.0093	0.0163	0.0488	0.1331	0.4658	1.8578	7.6569
40	0.0085	0.0147	0.0431	0.1169	0.4081	1.6269	6.7043
45	0.0078	0.0133	0.0386	0.1042	0.3630	1.4467	5.9604
50	0.0073	0.0122	0.0349	0.0940	0.3270	1.3027	5.3667

3. Performance Issues

What follows is a discussion of several issues impacting performance of a SAR.

3.1. Optimum Frequency

For this report, the optimum frequency band of operation is that which yields the maximum SNR in the image for the targets of interest.

For constant average transmit power, constant antenna aperture, constant resolution, constant velocity, and constant system losses, the SNR in the image is proportional to

$$\mathrm{SNR}_{\mathrm{image}} \quad \propto \quad f^{(n+1)} 10^{\frac{-\alpha|\boldsymbol{r}_s|}{10}} \quad , \tag{32}$$

where atmospheric loss rate α also depends on frequency (generally increasing with frequency.

Clearly, for any particular range $|\boldsymbol{r}_s|$, some optimum frequency exists to yield a maximum SNR in the image.

Figures 1 through 5 indicate the relative SNR in the image as a function of slant-range for various frequency bands.

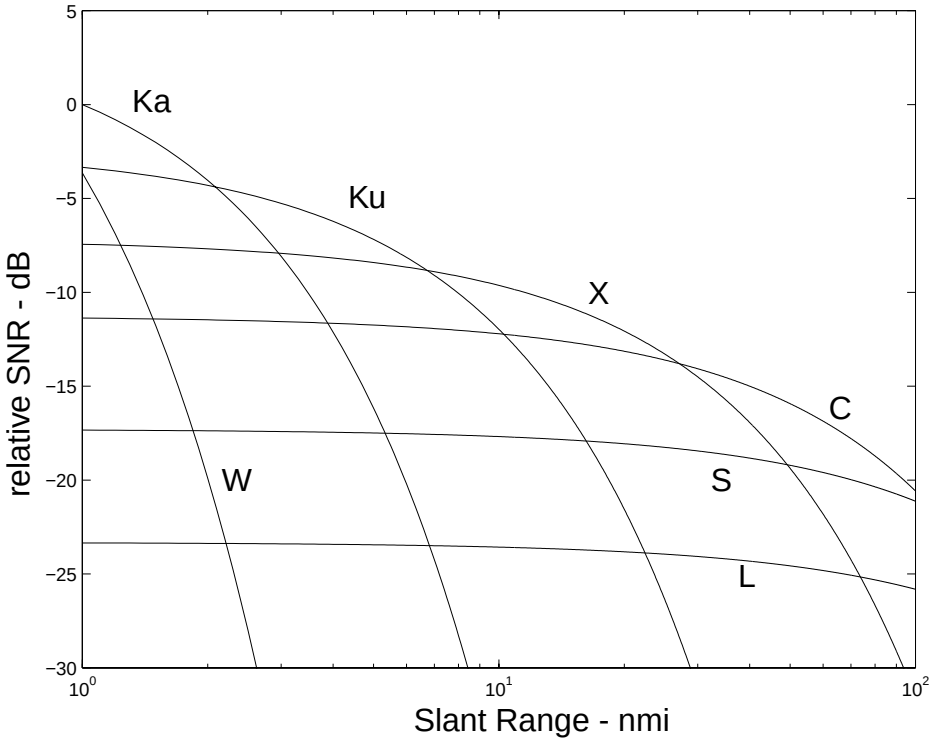

Figure 1. SAR relative performance of radar bands as a function of range (4 mm/Hr rain, 5 kft AGL altitude, n=1).

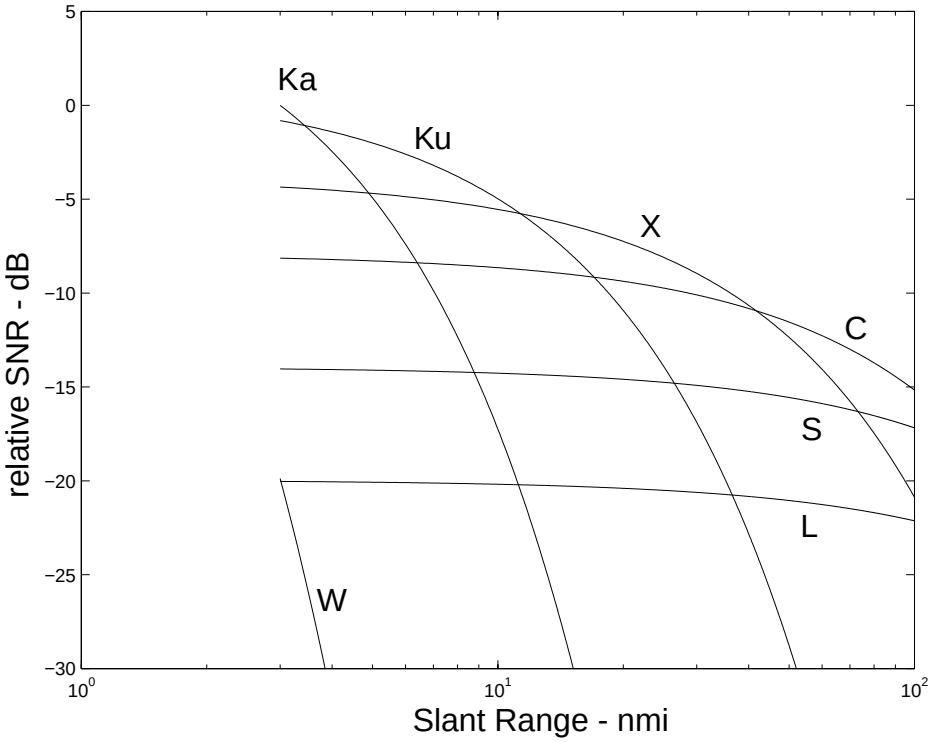

Figure 2. SAR relative performance of radar bands as a function of range (4 mm/Hr rain, 15 kft AGL altitude, n=1).

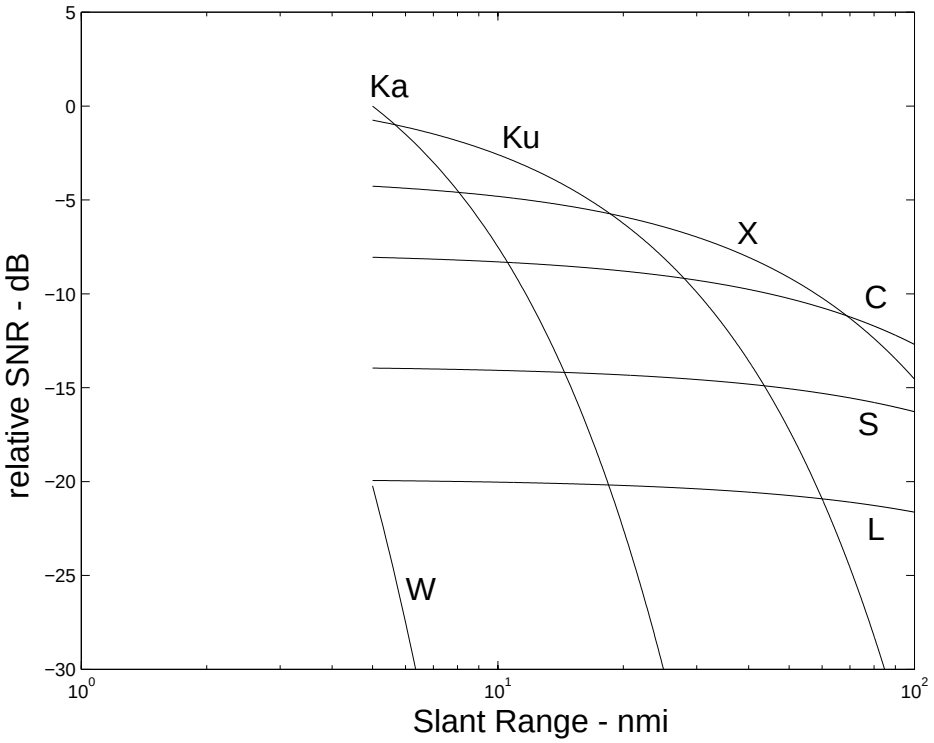

Figure 3. SAR relative performance of radar bands as a function of range (4 mm/Hr rain, 25 kft AGL altitude, n=1).

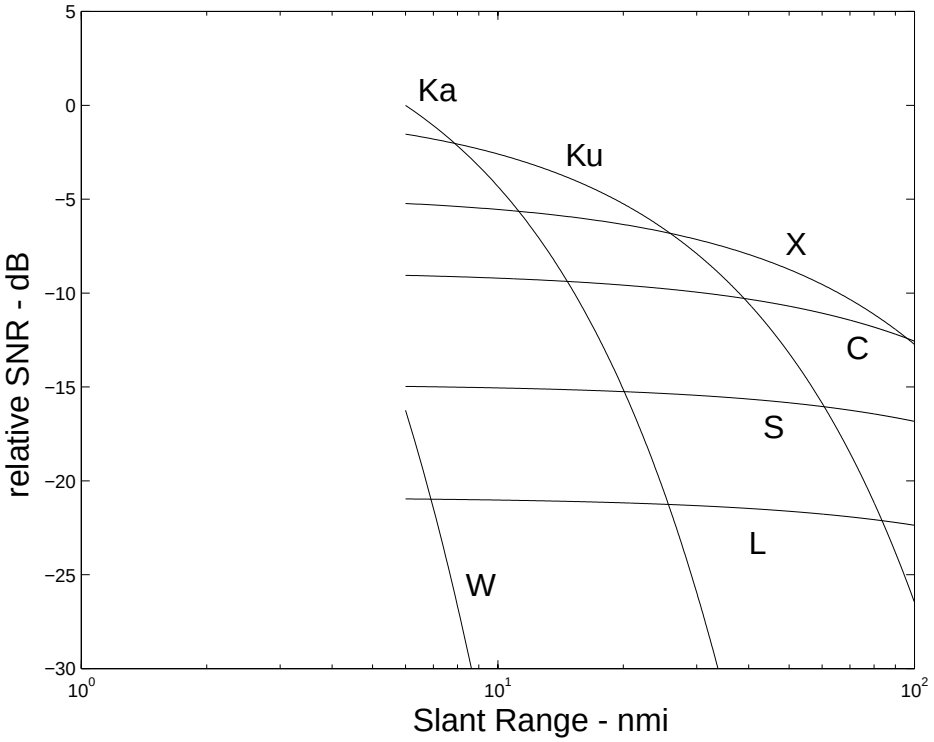

Figure 4. SAR relative performance of radar bands as a function of range (4 mm/Hr rain, 35 kft AGL altitude, n=1).

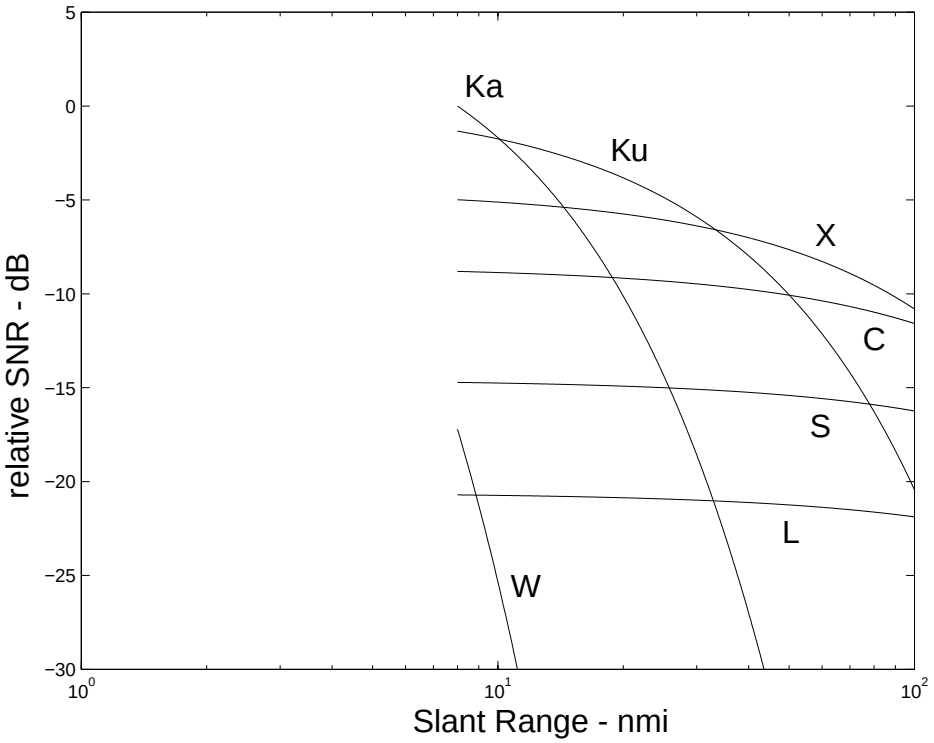

Figure 5. SAR relative performance of radar bands as a function of range (4 mm/Hr rain, 45 kft AGL altitude, n=1).

In summary, for a constant real antenna aperture size, antenna gain increases with frequency, as does brightness of the target. However, as range increases, atmospheric losses increase correspondingly and more so at higher frequencies, eventually overcoming any advantage due to antenna gain and target brightness. Consequently, for any particular atmosphere, radar height and range, there exists an optimum frequency band for SAR operation.

Generally, as range increases and/or weather gets worse, lower frequencies become more attractive.

Optimal frequencies for a typical SAR weather specification are illustrated in figure 6.

It should be noted that other reasons (besides optimal SNR) may exist for choosing a particular radar band for operation (e.g. spectral compatibility, pre-existing hardware, hardware availability, ATR template compatibility, managerial directive, etc.).

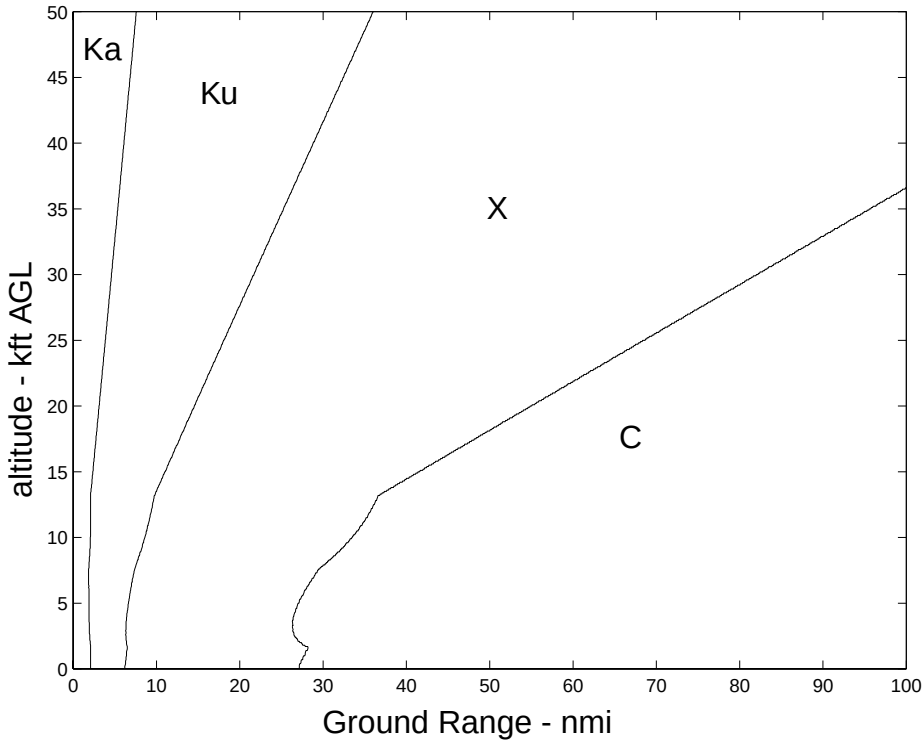

Figure 6. Optimum radar band as a function of range and altitude (4 mm/Hr rain, n=1, constant antenna aperture area).

3.2. PRF vs. Frequency

The Doppler bandwidth of a static scene is constrained by the antenna beamwidth to be

$$B_{\text{Doppler}} \approx \frac{2}{\lambda} v_x \theta_{\text{az}} \tag{33}$$

where

$$\theta_{\text{az}} = \text{antenna azimuth beamwidth (presumed to be small).} \tag{34}$$

The radar PRF is then chosen to be greater than this by some constant factor k_a, to limit aliasing, thereby yielding

$$f_p = k_a B_{\text{Doppler}} \ . \tag{35}$$

Typically, $k_a \geq 1.5$ to account for the antenna beam rolloff.

Noting that the antenna beamwidth is related to its physical aperture dimension D_{az} by

$$\theta_{\text{az}} \approx \lambda / D_{\text{az}} \tag{36}$$

yields the overall expression for PRF as

$$f_p \approx \frac{2 k_a v_x}{D_{\text{az}}} \ . \tag{37}$$

The interesting feature of this expression is that the radar PRF depends on the ratio of velocity to aperture dimension of the real antenna, but not on the radar wavelength. Consequently, for a fixed aperture size and velocity, the PRF is independent of frequency.

We note that Equation (36) is an approximate relationship between aperture dimension and beamwidth. A more precise relationship would depend on the actual aperture illumination characteristic, and probably yields a somewhat broader beam. Nevertheless, the underlying truth is that though Doppler is inversely proportional to wavelength, antenna beamwidth tends to be directly proportional to wavelength. Since these are multiplied to yield the total Doppler bandwidth observed in the antenna beam, they cancel in a manner to hold the total Doppler bandwidth constant over wavelength, thereby allowing a PRF independent of wavelength, as indicated in Equation (37).

3.3. Signal to Clutter in rain

While noise can obfuscate the SAR image, so too can competing echoes from undesired sources such as rain. Rain falling in the vicinity of a target scene will 'clutter' the image of that scene. For this analysis we identify the Signal-to-Clutter Ratio (SCR) as the ratio of signal energy (echo energy from a resolution cell of the target scene) to the clutter energy (echo energy from the rain processed into the same resolution cell of the target scene).

Raindrops are generally small with respect to a wavelength and nearly spherical, indicating Rayleigh scattering, but there are a whole lot of them. The volume reflectivity (RCS per unit volume) of rain is modeled by [6]

$$\sigma_V = (7 \times 10^{-12}) r^{1.6} f_{GHz}^4 \ \mathrm{m^2/m^3} \tag{38}$$

where

r = rain rate in mm/Hr,
f_{GHz} = frequency in GHz. (39)

This model agrees with measured data pretty well up to about Ka-band.[5] Tabulated values from this model are given in the following table.

Table 6: Rain volume reflectivity (dBm^{-1}) vs. rain rates

Rain Rate mm/Hr	L-band 1.5 GHz	S-band 3.0 GHz	C-band 5.0 GHz	X-band 9.6 GHz	Ku-band 16.7 GHz	Ka-band 35 GHz
0.25	–114	–102	–93	–82	–72	–59
1	–105	–92	–84	–72	–63	–50
4	–95	–83	–74	–63	–53	–40
16	–85	–73	–64	–53	–43	–31

Additionally, rain is not a static target, exhibiting its own motion spectrum. The motion spectrum typically is centered at some velocity with a recognizable velocity bandwidth. Data suggests a velocity bandwidth sometimes as high as 8 m/s, with a median velocity bandwidth of about 4 m/s.[4]

The RCS of a single resolution cell from the scene of interest is identified again as

$$\sigma_{\text{target}} = \frac{\sigma_{0,\,\text{ref}} \rho_a \rho_r}{\cos\psi} \left(\frac{f}{f_{\text{ref}}} \right)^n . \tag{40}$$

Correspondingly, the RCS of rain in a volume defined by the radar's resolution is

$$\sigma_{\text{rain}} = \sigma_V \rho_a \rho_r \rho_e \tag{41}$$

where

ρ_e = elevation resolution (limited by extent of rain height). (42)

We identify the elevation resolution as

$$\rho_e = \min\left(\frac{|\boldsymbol{r}_s| \sin\theta_{\text{el}}}{2}, \frac{h_r}{\cos\psi} \right) \tag{43}$$

where

θ_{el} = elevation beamwidth of the antenna, and

h_r = height extent of rain (typically 3 to 4 km). (44)

If the rain were static, that is, not moving at all, then the volume of rain would be completely coherent, as is the target resolution cell. In this case, the SCR due to rain is

$$\text{SCR}_{\text{rain}} = \frac{\sigma_{\text{target}}}{\sigma_{\text{rain}}}. \tag{45}$$

If the rain were completely noncoherent, then the rain response would not benefit from any coherent processing gain, much like thermal noise. In this case the SCR due to rain is increased to

$$\text{SCR}_{\text{rain}} = \frac{\sigma_{\text{target}}}{(a_w/N)\sigma_{\text{rain}}}. \tag{46}$$

In reality, rain is typically somewhere in-between completely coherent over an entire synthetic aperture, and completely non-coherent from pulse to pulse. Consequently we identify

$$\text{SCR}_{\text{rain}} = \frac{\sigma_{\text{target}}}{C\sigma_{\text{rain}}} \tag{47}$$

where C = the coherency factor for rain.

The rain coherency factor addresses the extent to which rain is coherent over the aperture collection time. If the rain is a coherent phenomena, then $C = 1$. If the rain is completely noncoherent, then $C = a_w/N$. In fact, rain is somewhere in-between completely and forever coherent, and completely noncoherent. We identify the rain coherency interval (time) as the inverse of the rain Doppler frequency bandwidth, which in turn depends on the rain's velocity bandwidth. Consequently, we identify

$$C = \frac{a_w T_{\text{rain coherence}}}{T_a} = \frac{a_w f_p}{N\left(\frac{2}{\lambda} B_{\text{Velocity}}\right)} \qquad \text{and } a_w/N \le C \le 1. \tag{48}$$

where

$T_{\text{rain coherence}}$ = rain coherence interval = $1/((2/\lambda)B_{\text{Velocity}})$,

B_{Velocity} = velocity bandwidth of rain in m/s, and

T_a = aperture collection interval = N / f_p. (49)

We note that for *C=1*, the rain is coherent and any single column of rain falls into a single resolution cell. For $C=a_w/N$, the rain is completely noncoherent and any single column of rain is smeared across all resolution cells.

Combining all the results yields

$$\text{SCR}_{\text{rain}} = \frac{\sigma_{\text{target}}}{C\,\sigma_{\text{rain}}} = \left(\frac{\sigma_{0,\text{ ref}}\left(\frac{f}{f_{\text{ref}}}\right)^n}{\sigma_V}\right)\left(\frac{\frac{N}{a_w}\left(\frac{2}{\lambda}B_{\text{Velocity}}\right)}{f_p \rho_e \cos\psi}\right) \tag{50}$$

where it is presumed that $a_w / N \le C \le 1$.

If we also assume ρ_e is limited by the antenna beam, and that $\sin\theta_{\text{el}} \approx \theta_{\text{el}} \approx \lambda / D_{\text{el}}$ where D_{el} is the antenna elevation aperture dimension, then

$$\text{SCR}_{\text{rain}} = \left(\frac{\sigma_{0,\text{ ref}}}{\sigma_V}\right)\left(\frac{f}{f_{\text{ref}}}\right)^n\left(\frac{4ND_{\text{el}}B_{\text{Velocity}}}{\lambda^2 a_w f_p |\boldsymbol{r}_s| \cos\psi}\right) = \left(\frac{\sigma_{0,\text{ ref}}}{\sigma_V}\right)\left(\frac{f}{f_{\text{ref}}}\right)^n\left(\frac{2D_{\text{el}}B_{\text{Velocity}}}{\lambda \cos\psi \rho_a v_x}\right) \tag{51}$$

or, plugging in the rain volume reflectivity

$$\text{SCR}_{\text{rain}} = \left(\frac{\sigma_{0,\text{ ref}}}{f_{\text{ref}}^n}\right)\left(\frac{1}{3.5\times 10^{-48}}\right)\left(\frac{D_{\text{el}}B_{\text{Velocity}}}{f^{(3-n)} r^{1.6} c \rho_a v_x \cos\psi}\right). \tag{52}$$

Clearly, SCR due to rain gets worse at higher frequencies, heavier rain rates, coarser resolutions, and higher platform velocities. Just how bad is it? The following tables quantify some SCRs.

Table 7: SCR_{rain} (dB) for 1 m resolution at v_x = 50 m/s, ($\sigma_{0,\text{ref}}$ = –25 dB at f_{ref} = 16.7 GHz, D_{el} = 0.2 m, B_{Velocity} = 4 m/s)

Rain Rate mm/Hr	L-band 1.5 GHz	S-band 3.0 GHz	C-band 5.0 GHz	X-band 9.6 GHz	Ku-band 16.7 GHz	Ka-band 35 GHz
0.25	71	65	61	55	50	44
1	62	56	51	46	41	35
4	52	46	42	36	31	25
16	42	36	32	26	22	15

Table 8: SCR_{rain} (dB) for 10 m resolution at v_x = 280 m/s ($\sigma_{0,ref}$ = –25 dB at f_{ref} = 16.7 GHz, D_{el} = 0.2 m, $B_{Velocity}$ = 4 m/s)

Rain Rate mm/Hr	L-band 1.5 GHz	S-band 3.0 GHz	C-band 5.0 GHz	X-band 9.6 GHz	Ku-band 16.7 GHz	Ka-band 35 GHz
0.25	54	48	43	38	33	26
1	44	38	34	28	23	17
4	34	28	24	18	13	7.2
16	25	19	14	8.8	4.0	–2.4

Since a typical SAR noise specification in the image is equivalent to a target scene reflectivity of –25 dB at Ku-band, we note from the tables that we expect rain to be noticeable only for the worst rain rates, at the highest frequencies, at extremely coarse resolutions, and at substantial velocities. Nevertheless, while most airborne SARs do not, some SARs do in fact operate under these conditions which warrants a cursory check of rain clutter sensitivity. After all, radar is touted as an all/adverse-weather sensor.

3.4. Pulses in the Air

Typical operation for terrestrial airborne SARs is to send out a pulse and receive the expected echoes before sending out the subsequent pulse. This places constraints on range vs. velocity parameters for the SAR.

We continue with the presumption that the effective pulse width of the SAR is equal to the actual transmitted pulse width. For matched-filter pulse compression this is the case, and for ‘stretch’ processing (deramping followed by a frequency transform) this is nearly the case and more so for small scene extents compared with the pulse width.

By insisting that the echo return before the subsequent pulse is emitted, we insist that

$$\left(T_{eff} + \frac{2}{c}|\boldsymbol{r}_s|\right) \le \frac{1}{f_p} \tag{53}$$

which can be manipulated to

$$|\boldsymbol{r}_s| \le \frac{c(1-d)}{2f_p} \tag{54}$$

and furthermore to

$$|\boldsymbol{r}_s| \le \frac{c(1-d)D_{\text{az}}}{4k_a v_x} \tag{55}$$

The maximum $|\boldsymbol{r}_s|$ that satisfies this expression is often referred to as the ‘unambiguous

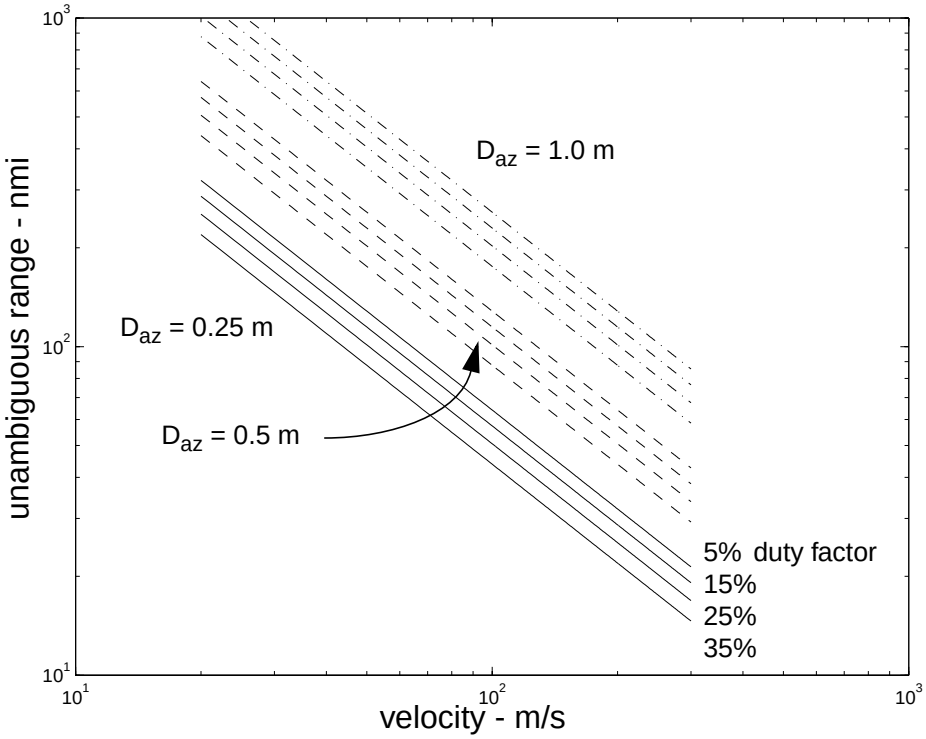

Figure 7. Unambiguous range limits for k_a=1.5.

range' of the SAR. We note that the unambiguous range decreases with increasing velocity, increasing duty factor, and increasing k_a. The unambiguous range increases with a larger real antenna aperture azimuth dimension. Furthermore, the unambiguous range is frequency independent (for constant real apertures).

Figure 7 plots unambiguous range vs. velocity for several duty factors and antenna dimensions.

If we need to work at a range beyond the unambiguous range, we need to either extend the unambiguous range (by appropriately modifying the radar antenna, duty factor, velocity, or oversampling factor k_a), or we need to operate with pulses 'in the air', that is, transmitting new pulses before the expected arrival of a previous pulse's echo. This is entirely possible and is in fact routine in space-based SAR (where often perhaps a dozen or more pulses are transmitted prior to receiving an echo from the first pulse).

3.5. Extending Range

Extending the range of a SAR is equivalent to

1) ensuring that an adequate SNR is achievable at the new range of interest, and
2) ensuring that the unambiguous range constraint is adequately dealt with.

The unambiguous range issue was addressed in the last section. Here we address methods for increasing SNR at some range of interest.

We begin by recalling the expression for SNR in the SAR image, that is

$$\mathrm{SNR}_{\mathrm{image}} = \frac{P_{\mathrm{avg}}(\eta_{\mathrm{ap}}^2 A_A^2)\rho_r \left(\frac{\sigma_{0,\,\mathrm{ref}}}{f_{\mathrm{ref}}^n}\right)(f)^{n+1}}{(8\pi)a_w ckTv_x(L_{\mathrm{sp}}L_{\mathrm{radar}}F_N)\left(|\boldsymbol{r}_s|^3\sqrt{1-(h/|\boldsymbol{r}_s|)^2}\,10^{\frac{\alpha|\boldsymbol{r}_s|}{10}}\right)}. \tag{56}$$

A discussion of increasing SNR needs to examine what we can do with the individual parameters within the equation.

Increasing Average TX Power

We recall that the average TX power is the product of the peak TX power and the duty factor of the radar. Obviously we can increase the average power by increasing either one of these constituents, as long as it is not at the expense of the other. For example, a 100-W power amplifier operating at 30% duty factor is still better than a 200-W power amplifier operating at only a 10% duty factor, as far as SNR is concerned.

For a given TX power amplifier operating at full power, all we can do is ensure that we are operating at or near its duty factor limit. Since

$$P_{\mathrm{avg}} = P_t d = P_t T_{eff} f_p \tag{57}$$

this is accomplished by increasing either or both the pulse width T_{eff} and the radar PRF f_p. If the radar PRF is constrained by an unambiguous range requirement, then the pulse width must be extended. For fine resolution SARs employing stretch processing we identify

$$T_{eff} = I / f_s \tag{58}$$

where

I = the total number of (fast-time) samples collected from a single pulse, and
f_s = the ADC sampling frequency employed. (59)

We note that to satisfy Nyquist criteria using quadrature sampling,

$$f_s \geq B_{\mathrm{IF}} \tag{60}$$

where B_{IF} is the IF bandwidth of the SAR.

Consequently, increasing the pulse width requires either collecting more samples *I*, or decreasing the ADC sampling frequency f_s (and the corresponding IF filter bandwidth B_{IF}).

Two important issues need to be kept in mind, however. The first is that extending the pulse width restricts the nearest range that the radar can image. That is, the TX pulse has to end before the near range echo arrives. The second is that the number of samples *I* restricts the range swath of the SAR image to $(B_{\mathrm{IF}} / f_s)I$ resolution cells. The consequence to this is that relatively wide swaths at near ranges requires lots of samples *I* at very fast ADC sampling rates with corresponding wide IF filter bandwidths.

At far ranges, where near-range timing is not an issue, for a fixed IF filter bandwidth and ADC sampling frequency, we can always increase pulse width by collecting more samples *I*. If operating near the unambiguous range, however, prudence dictates that we remain aware that increasing the duty factor does in fact reduce the unambiguous range somewhat.

Operating beyond the unambiguous range limit requires a careful analysis of the radar timing in order to maximize the duty factor, juggling a number of additional constraints. It's enough to make your head spin.

Stretch processing derives no benefit from a duty factor greater than about 50%. A reasonable limit on usable duty factor due to other timing issues is often in the neighborhood of about 35%.

In any case, the easiest retrofit to existing SARs for increasing average TX power (and hence range) are first to increase the PRF to the maximum allowed by the timing, and second to increase the number of samples collected.

Furthermore, we note that at times it may be advantageous to shorten the pulse and increase the PRF, even if it means operating with pulses in the air (beyond the reduced unambiguous range), just to increase the duty factor. This is particularly true when the hardware is limited in how long a pulse can be transmitted.

Increasing Antenna Area

A bigger antenna (in either dimension) and/or better efficiency will yield improved SNR.

The down side is that a bigger azimuth dimension to the antenna aperture will restrict continuous strip mapping to coarser resolutions by the well known equation

$$\rho_a \geq D_{\mathrm{az}} / 2 \qquad \text{(for strip mapping).} \tag{61}$$

Furthermore a bigger elevation dimension for the antenna aperture will reduce the illuminated range swath, thereby restricting perhaps the imaged range swath, especially at steeper depression angles.

However, we note that in the SNR equation, antenna area and efficiency are squared. Consequently, doubling either one of these is equivalent to four times an increase in average TX power.

Selecting Optimal Frequency

As previously discussed, there is a clear preference for operating frequency depending on range, altitude, and weather conditions. For example, at a 50-nmi range from a 25-kft AGL altitude with 4 mm/Hr rain, X-band offers a 12.9 dB advantage over Ku-band. For perspective, a 1-kW Ku-band amplifier would provide performance equivalent to a 51-W X-band amplifier (for the same real antenna aperture, efficiency, yadda, yadda, yadda....).

Choice of operating frequency does need to be tempered, however, by the factors noted earlier in this report.

Interestingly, there may even be significant differences within the same radar band. For example, at 25 kft AGL altitude, within the international Ku-band (15.7 GHz to 17.7 GHz) the bottom edge provides 1.25 dB better SNR than the top edge at 20 nmi, 2.4 dB better SNR at 30 nmi, 3.5 dB better performance at 40 nmi, and 4.7 dB better performance at 50 nmi. Clearly, it seems advantageous to operate as near to the optimum frequency as the hardware and frequency authorization allow.

Modifying Operating Geometry

Once above the water-cloud layer, increasing the radar altitude will generally yield reduced average atmospheric attenuation, and hence improved transmission properties for a given range. Consequently, SNR is improved with operation at higher altitudes for any particular typical weather condition.

This translates to increased range at higher altitudes.

Coarser Resolutions

SNR is directly proportional to slant-range resolution. However in the radar equation as presented, no overt effect is obvious due to changing azimuth resolution. This is because as azimuth resolution gets finer, the target cell RCS diminishes as expected, but also the synthetic aperture lengthens correspondingly thereby increasing coherent processing gain and exactly countering the effects of diminished RCS. The net effect is no change to SNR.

Consequently, only slant-range resolution influences SNR.

The next several figures illustrate how range-performance in both clear air and adverse weather depends on operating geometry and resolution. Acceptable SNR performance is achievable to the left of the curves corresponding to a particular resolution.

We note that 1 nmi (nautical mile) = 1.852 kilometers, and 1 kft = 304.8 meters. Furthermore, 1 kt = 0.514444 m/s approximately.

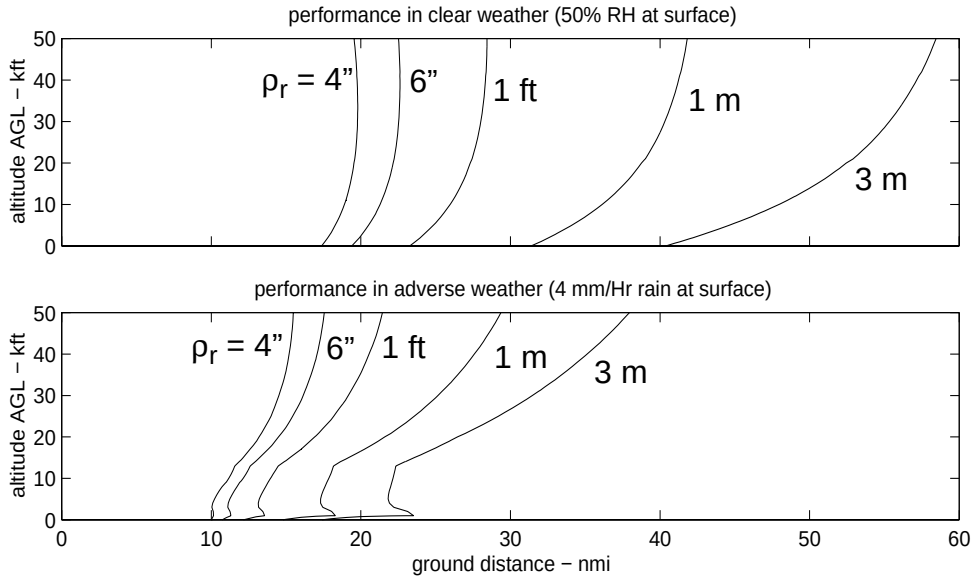

Frequency = 16.7 GHz
Power (peak) = 320 W
duty factor = 0.35
Antenna (ap area) = 93.0002 sq in
Antenna (ap efficiency) = 0.5

Velocity (ground speed) = 70 kts
Noise reflectivity = −25 dB
Losses (signal processing) = 2 dB
Losses (radar) = 2 dB
Noise figure = 4 dB

Figure 8. Geometry limits vs. resolution.

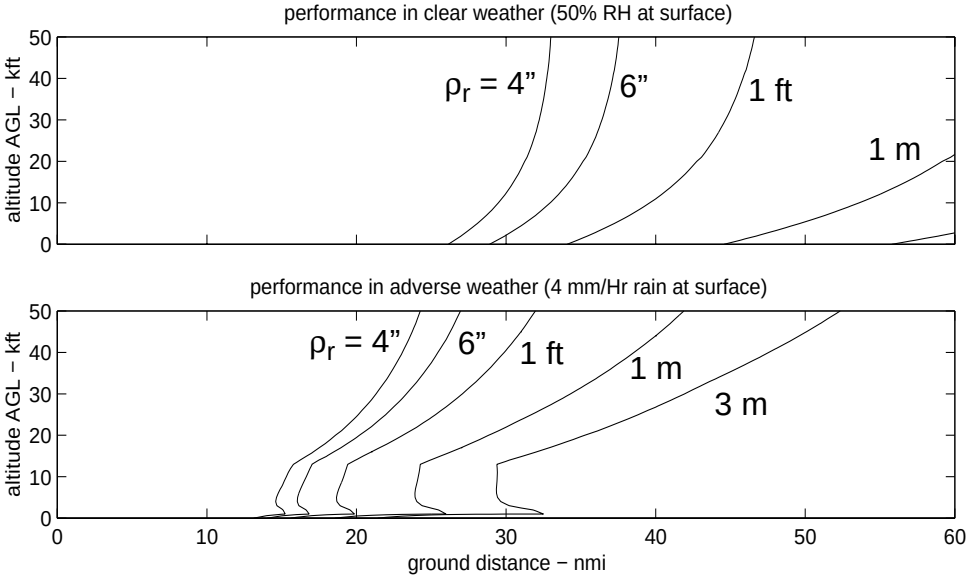

Frequency = 16.7 GHz
Power (peak) = 700 W
duty factor = 0.35
Antenna (ap area) = 297 sq in
Antenna (ap efficiency) = 0.43

Velocity (ground speed) = 250 kts
Noise reflectivity = −25 dB
Losses (signal processing) = 2 dB
Losses (radar) = 2.7 dB
Noise figure = 3.2 dB

Figure 9. Geometry limits vs. resolution.

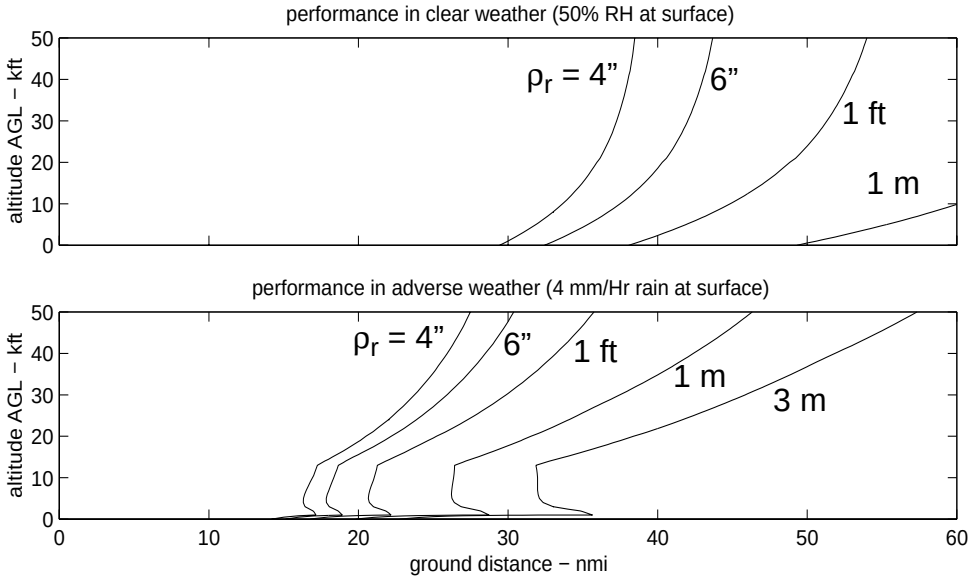

Frequency = 16.7 GHz
Power (peak) = 700 W
duty factor = 0.35
Antenna (ap area) = 576 sq in
Antenna (ap efficiency) = 0.43

Velocity (ground speed) = 580 kts
Noise reflectivity = −25 dB
Losses (signal processing) = 2 dB
Losses (radar) = 2.7 dB
Noise figure = 3.2 dB

Figure 10. Geometry limits vs. resolution.

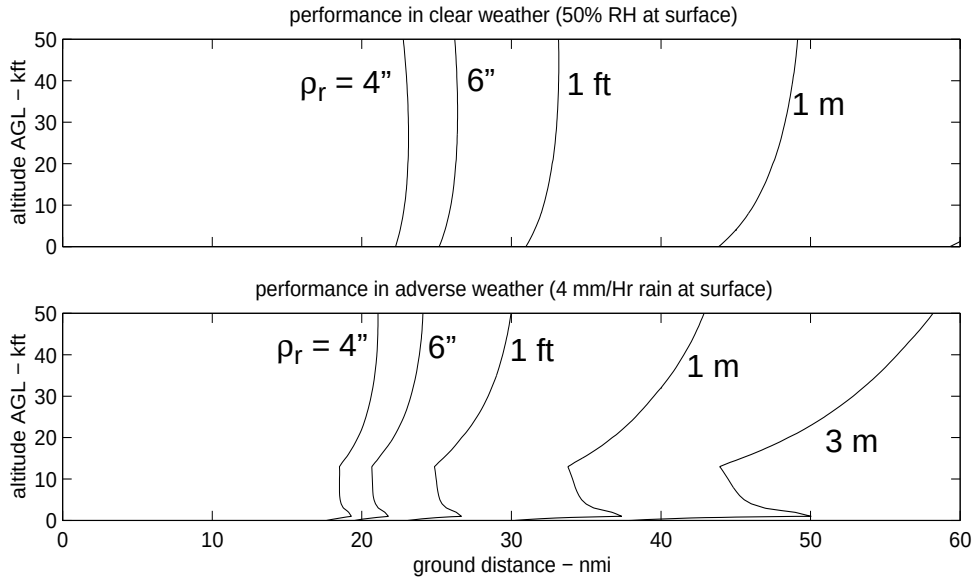

Frequency = 9.6 GHz
Power (peak) = 350 W
duty factor = 0.35
Antenna (ap area) = 178.2504 sq in
Antenna (ap efficiency) = 0.47

Velocity (ground speed) = 100 kts
Noise reflectivity = −25 dB
Losses (signal processing) = 2 dB
Losses (radar) = 2 dB
Noise figure = 4 dB

Figure 11. Geometry limits vs. resolution.

Decreasing Velocity

SNR is really a function of the total energy collected from the target scene. Total energy, of course, is the average power integrated over the aperture time. Consequently, a longer aperture time yields a better SNR. We achieve a longer aperture time for a fixed aperture length by flying slower, that is, collecting data at a reduced velocity. Hence, collecting data at a slower velocity allows a greater SNR in the image, due to a greater coherent integration gain.

However, what is important is not the actual velocity of the aircraft, but rather the translational velocity v_x defined to be the horizontal velocity orthogonal to $|\boldsymbol{r}_s|$. If the aircraft is traveling in a direction not horizontal and orthogonal to $|\boldsymbol{r}_s|$, then the important parameter v_x is that component of the aircraft velocity that is. This brings in the notion of 'squint' angle, illustrated in figure 12.

The aircraft might be flying with a velocity v_{aircraft}, but with a squint angle θ_{squint} and pitch angle ϕ_{pitch} with respect to the target. The velocity component of interest, that is, the velocity component that influences SNR is

$$v_x = v_{\text{aircraft}} \cos\phi_{\text{pitch}} \sin\theta_{\text{squint}} \tag{62}$$

where

v_{aircraft} = the magnitude of the aircraft velocity vector,
ϕ_{pitch} = the pitch angle of the velocity vector, and

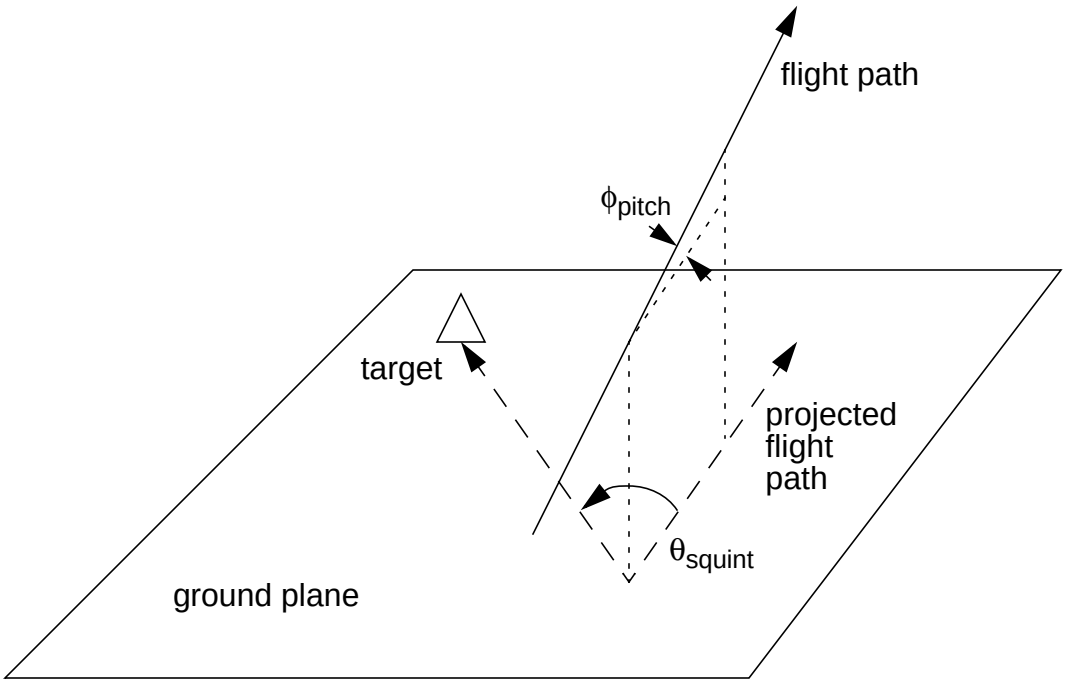

Figure 12. Flight path geometry definitions.

θ_{squint} = the squint angle to the target (as projected on the ground). (63)

Nominally, SAR collects data from a level flight path ($\phi_{pitch} = 0$), and a broadside geometry ($\theta_{squint} = 90°$). Clearly, one way to reduce the velocity component v_x is to squint forward sufficiently. For example, at $\theta_{squint} = 45°$, we calculate $v_x = 0.707 v_{aircraft}$, with a corresponding potential increase in SNR of 1.5 dB.

This improves much more for more severe squint angles. The down side to more severe squint angles are more severe geometric distortions in the SAR image, and an increase in required bandwidth.[2, 3]

It is also important to note that unambiguous range is extended with a reduced v_x.

Another way to effectively increase the total aperture time (and hence SNR) is to coherently combine data from multiple collection passes. Noncoherent integration of distinct SAR images can also offer improvement.

Decreasing Radar Losses, Signal Processing Losses, and System Noise Factor

Any reduction in system losses yields a SNR gain of equal amount. This is also true of reducing the system noise factor. For example, reducing the TX amplifier to antenna loss by 1 dB translates to a 1-dB improvement in SNR. Likewise, a 2-dB reduction in system noise factor translates to a 2-dB improvement in SNR.

We note that high-power devices such as duplexers, switches, and protection devices tend to be lossier than lower power devices. Consequently, doubling the TX power amplifier output power might require lossier components elsewhere in the radar, rendering less than a doubling of SNR in the image. Furthermore, high-power microwave switches tend to be bulkier than their low-power counterparts, requiring perhaps longer switching times which may impact achievable duty factors.

Easing Weather Requirements

Atmospheric losses are less in fair weather than in inclement weather. Consequently SNR is improved (and range increased) for a nicer atmosphere. In real life you get what you get in weather, although a data collection might make use of weather inhomogeneities (like choosing a flight path or time to avoid the worst conditions).

Weather attenuation models are very squishy (of limited accuracy) and prone to widely varying interpretations. Consequently, SAR performance claims might use this to advantage (and probably often do). The point of this is that while requests for proposals often contain a weather specification/requirement (e.g. 4 mm/Hr rain over a 10 nmi swath), there is no uniform interpretation on what this means insofar as attenuation to radar signals.

Changing Reference Reflectivity

This is equivalent to the age-old technique of "If we can't meet the spec, then reduce the spec."

We note that a radar that meets the common requirement of a 0-dB SNR with $\sigma_{0,\,\mathrm{ref}} = -25$ dB at some range, will meet a 0-dB SNR for $\sigma_{0,\,\mathrm{ref}} = -20$ dB at some farther range. SNR performance tends to degrade gracefully with range, consequently a tolerance for poorer image quality will result in longer range operation.

The equivalent reflectivity of the noise in the SAR image is denoted as σ_N. That is,

$$\sigma_N = \sigma_0\big|_{\mathrm{SNR_{image}} = 0\ \mathrm{dB}}. \tag{64}$$

The following figures illustrate how artificially degrading the SNR in the image (by effectively increasing σ_N) affects image quality for a Ku-band SAR image of the Capitol building in Washington, DC.

Depending on what we might be looking for, even fairly noisy images can still be usable. For example, the Capitol dome is still identifiable even with $\sigma_N = -15$ dB.

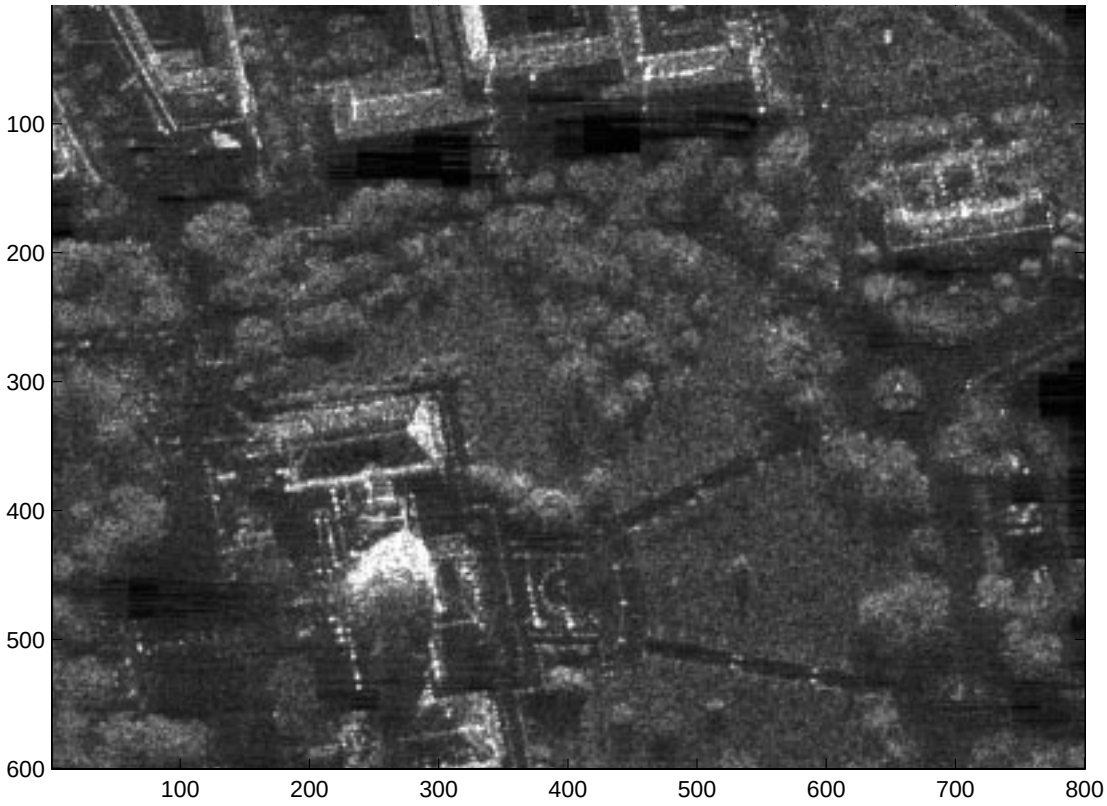

Figure 13. Untouched Ku-band SAR Image with $\sigma_N < -30$ dB.

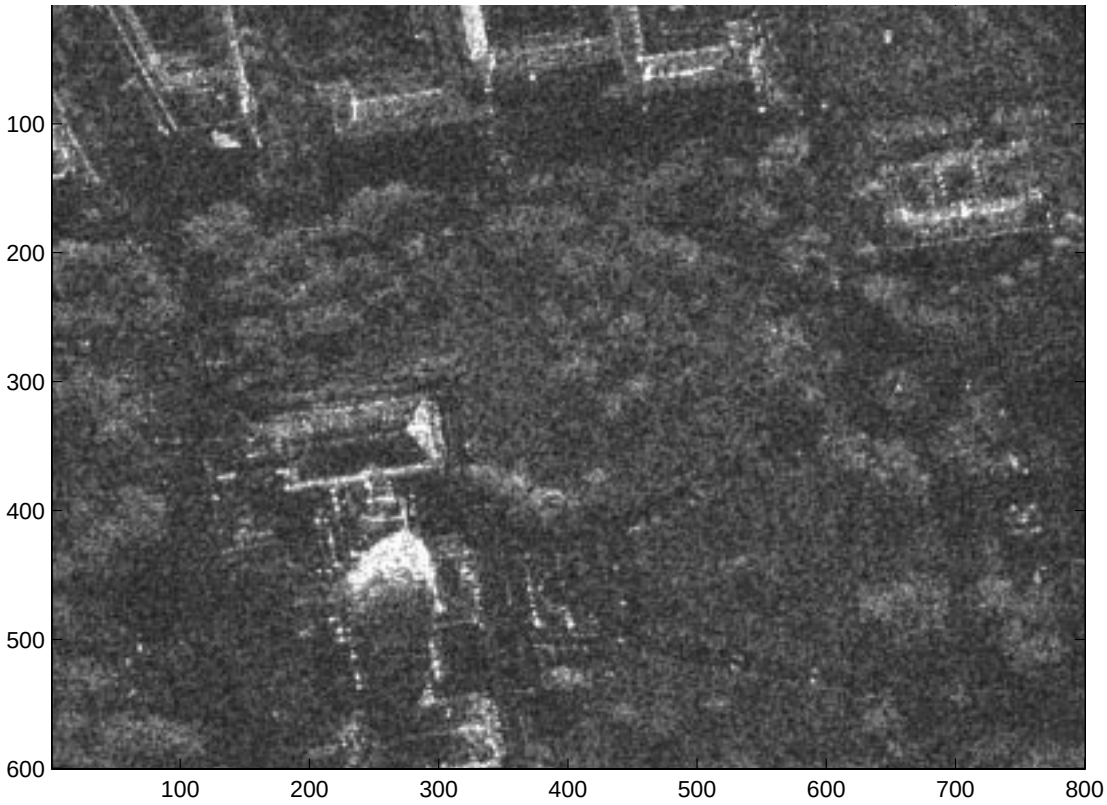

Figure 14. SAR Image with simulated $\sigma_N = -25$ dB.

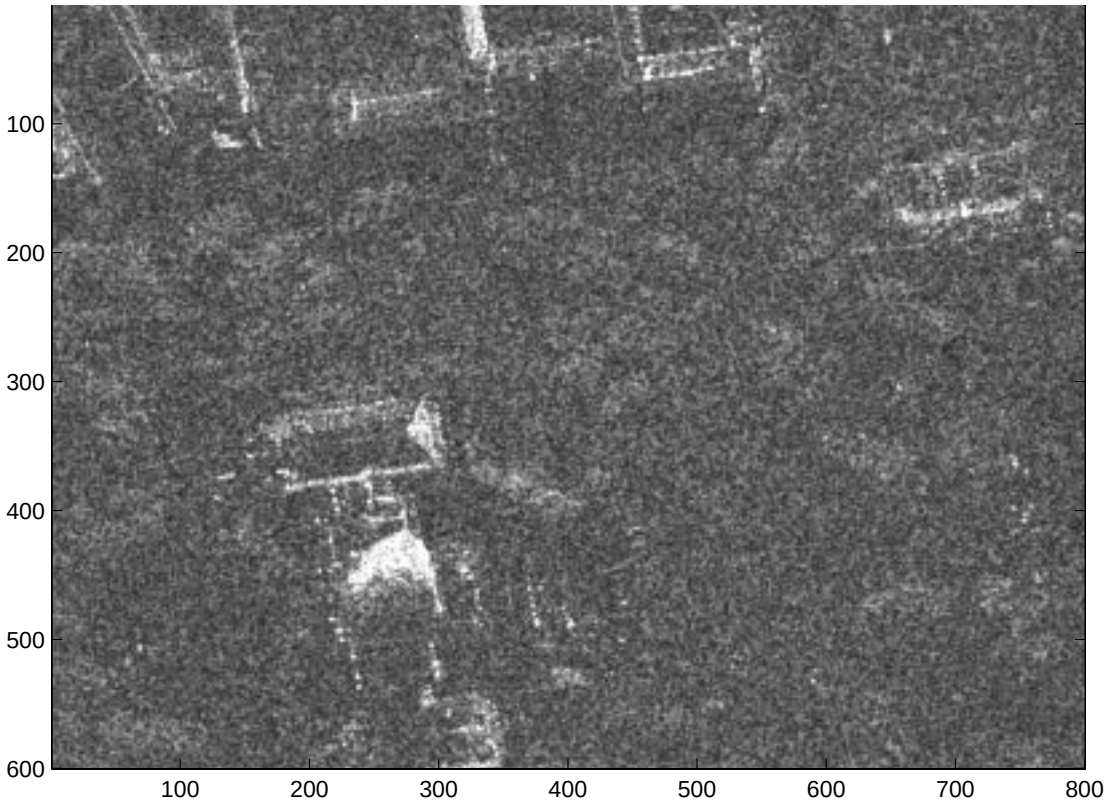

Figure 15. SAR Image with simulated $\sigma_N = -20$ dB.

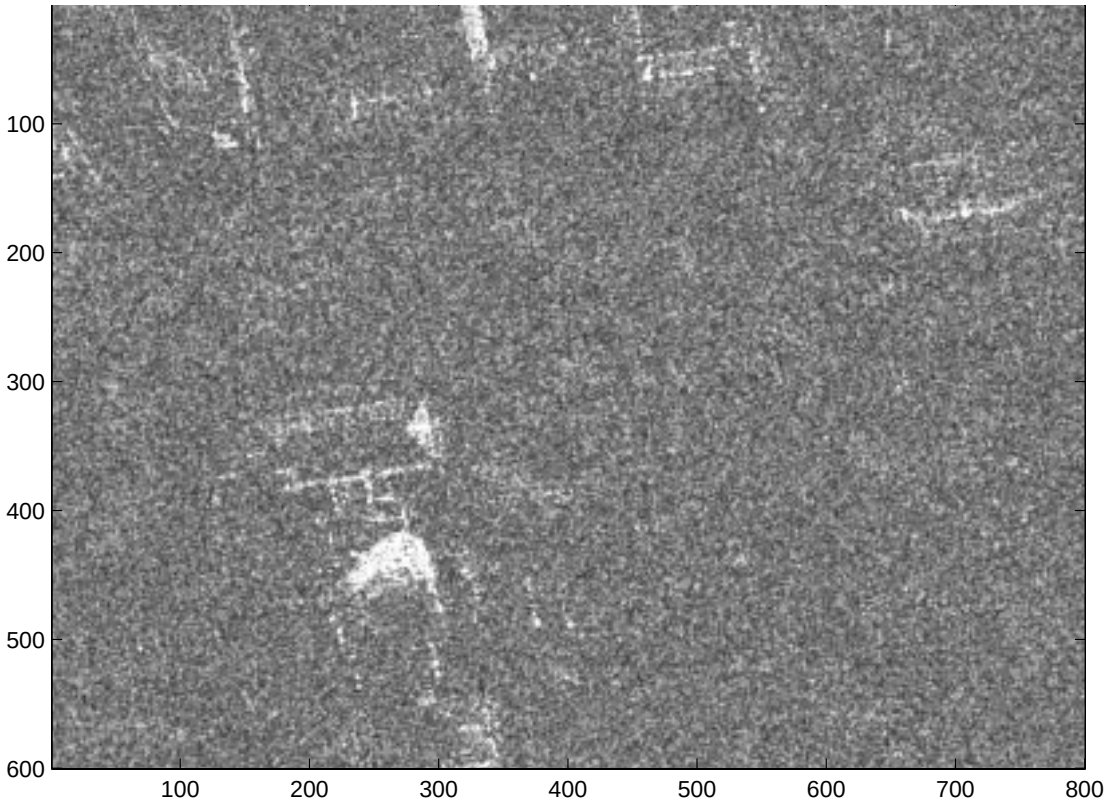

Figure 16. SAR Image with simulated $\sigma_N = -15$ dB.

4. Conclusions

The aim of this report is to allow the reader to understand the nature of relevant physical parameters in how they influence SAR performance. The radar equation can be (and was) transmogrified to a form that shows these parameters explicitly. Maximizing performance of a SAR system is then an exercise in modifying the relevant parameters to some optimum combination. This was discussed in detail.

Nevertheless, some observations are worth repeating here.

- For lots of power over wide bandwidths, active phased arrays look like the way to go. Current technology offers 10 W per square centimeter at X-band. Experimental MMICs are already demonstrating many tens of Watts at Ku-band.
- Atmospheric losses are typically greater at higher frequency, in heavier rainfalls, and at lower altitudes. These conspire to indicate an optimum operating frequency for a constrained antenna area at any particular operating geometry and weather condition.
- For a fixed antenna size, optimum PRF is independent of radar frequency.
- The direct return from rain should not generally be a problem in a typical SAR image, unless we are flying really fast and imaging at the higher radar frequencies at relatively coarse resolutions in particularly heavy rain.
- Imaging at long ranges from high velocities will necessitate pulses in the air. This is made worse by small antenna dimensions, and higher duty factors.
- Extending the range of a SAR system can be done by incorporating any of the following:

  increasing average TX power (peak TX power and/or duty factor)
  increasing antenna area and/or efficiency
  operating in a more optimal radar band (or portion of a radar band)
  flying at a more optimal altitude (usually higher)
  operating with coarser range resolution (azimuth resolution doesn’t help)
  decreasing tangential velocity (decreasing velocity, or more severe squint angles)
  decreasing system losses and/or system noise factor
  operating in more benign weather conditions
  degrading the noise equivalent reflectivity required of the scene

Bibliography

[1] Doerry, Armin W., “Atmospheric Loss Model for Lynx SAR”, internal informal memo to Distribution, October 13, 1997.

[2] Doerry, Armin, “Bandwidth requirements for fine resolution squinted SAR”, SPIE 2000 International Symposium on Aerospace/Defense Sensing, Simulation, and Controls, Radar Sensor Technology V, Vol. 4033, Orlando FL, 27 April 2000.

[3] Doerry, Armin W., “Squint Mode SAR in 3-D”, internal informal memo to Distribution, September 18, 1997.

[4] Doviak, Richard J., Dusan S. Zrnic, “Doppler Radar and Weather Observations” - second edition, ISBN 0-12-221422-6, Academic Press, Inc., 1993.

[5] Nathanson, Fred E., “Radar Design Principles” - second edition, ISBN 0-07-046052-3, McGraw-Hill, Inc., 1991.

[6] Skolnik, Merrill I., “Introduction to Radar Systems” - second edition, ISBN 0-07-057090-1, McGraw-Hill, Inc., 1980.

atmrate2
snrvsf.m
optimalf.m
raincltr.m
snrvsgeo.m
resvsgeo.m

Distribution

1	MS 0529	B. C. Walker	2308
1	MS 0519	G. Kallenbach	2345
2	MS 0519	A. W. Doerry	2345
1	MS 0519	D. F. Dubbert	2345
1	MS 0519	S. S. Kawka	2345
1	MS 0519	G. R. Sloan	2345
1	MS 0519	B. L. Remund	2348
1	MS 0519	T. P. Bielek	2348
1	MS 0519	B. L. Burns	2348
1	MS 0519	S. M. Devonshire	2348
1	MS 0519	J. A. Hollowell	2348
1	MS 0519	M. S. Murray	2348
1	MS 0519	J. W. Redel	2348
1	MS 0537	R. M. Axline	2344
1	MS 0537	D. L. Bickel	2344
1	MS 0537	J. T. Cordaro	2344
1	MS 0537	W. H. Hensley	2344
1	MS 0519	Ana Martinez	2346
1	MS 0537	Bobby Rush	2331
1	MS 1207	C. V. Jakowatz, Jr.	5912
1	MS 1207	P. H. Eichel	5912
1	MS 9018	Central Technical Files	8945-1
2	MS 0899	Technical Library	9616
1	MS 0612	Review & Approval Desk for DOE/OSTI	9612

;-)